



ELSEVIER

Catena 44 (2001) 111–132

**CATENA**

www.elsevier.com/locate/catena

# Weathering of a gypsum-calcareous mudstone under semi-arid environment at Tabernas, SE Spain: laboratory and field-based experimental approaches

Yolanda Cantón<sup>a</sup>, Albert Solé-Benet<sup>a,\*</sup>, Ignasi Queralt<sup>b</sup>,  
Roberto Pini<sup>c</sup>

<sup>a</sup> Estación Experimental de Zonas Áridas, CSIC, General Segura 1, 04001 Almería, Spain

<sup>b</sup> Institut de Ciències de la Terra “Jaume Almera”, CSIC, Solé i Sabarís s/n, 08028 Barcelona, Spain

<sup>c</sup> Istituto per la Chimica del Terreno, CNR, Via Alfieri 1, 5600 Ghezzano (Pisa), Italy

Received 22 February 2000; received in revised form 24 July 2000; accepted 6 September 2000

## Abstract

The weathering of a Late Miocene gypsum-calcareous mudstone outcropping in large badland areas of SE Spain, under a semi-arid Mediterranean climate, was studied by means of two experimental approaches. Field and laboratory experiments were carried out to reproduce, though in accelerated form, some of the weathering conditions of the consolidated mudstone. In the laboratory, three sequences of 5, 10 and 20 wetting–drying cycles were produced on undisturbed blocks of fresh mudstone samples. At the end of the three sequences, samples were analysed for their micromorphology, elemental and soluble salt chemistry, and total mineralogy. Unweathered dry samples, as blanks, and permanently wet samples were also analysed. In the field, two small plots of freshly exposed mudstone were monitored over 3 years for their response to natural weathering in terms of morphological changes and sediment output. The porosity was increased by a few wetting–drying cycles, as assessed by significant increases in water absorption capacity of the mudstone. A combination of three factors is responsible for mudstone weathering: repeated cycles of wetting–drying, the presence of geologically-induced cracks and fissures, and dissolution–crystallisation of relatively soluble minerals, gypsum being the most abundant within this category. A few wetting–drying cycles were sufficient to reveal ion migration (specially  $\text{Na}^+$ ,  $\text{Ca}^{++}$ ,  $\text{Mg}^{++}$ ,  $\text{SO}_4^-$ ,  $\text{HCO}^-$  and  $\text{Cl}^-$ ) within the mudstone, explaining mineral dissolution. In the field, surface weathering rates from 0.7 to 8 mm year<sup>-1</sup> were measured. Weathering rates were found to be proportional to the number of rainfall events during the sampling periods, confirming what was found in laboratory conditions, namely, that the number of wetting–drying cycles has

\* Corresponding author. Fax: +34-950-277-100.

E-mail address: albert@eeza.csic.es (A. Solé-Benet).

the greatest influence on weathering. These weathering rates might be considered as the probable range of incision rates under present semi-arid conditions. © 2001 Elsevier Science B.V. All rights reserved.

*Keywords:* Gypsum; Weathering; Porosity; Erosion rates; Badlands; Migration of elements

## 1. Introduction

In the Tabernas “desert”, near the town of Tabernas, in Almeria province (SE Spain), an extensive landscape of badlands, receiving less than 200 mm of annual rainfall, has developed over a quite homogeneous and monotonous series of gypsum-calcareous mudstones (Kleverlaan, 1989; Alexander et al., 1994; Calvo-Cases et al., 1991a,b; Calvo and Harvey, 1996). Most studies from this badland area consider erosion to be dependent on sediment availability rather than on runoff rates (Calvo-Cases et al., 1991a,b; Solé-Benet et al., 1997).

According to Carson and Kirkby (1972, cited by Campbell, 1989), geomorphological processes on hillslopes are either weathering-limited or transport-limited and critical limits can be set by the comparative rates of weathering and erosion: where weathering predominates a weathered mantle forms and such slopes or surfaces are then transport-limited; where the rate of erosion is greater, weathered debris do not accumulate and a weathering-limited condition exists.

The perception of high erosion rates is often assumed on the basis of a badland morphology. Nevertheless, previous studies in the Tabernas area indicate that present rates of erosion are in general very low, due in part to the scarcity of precipitation. However, rates can be very high locally, especially in the absence of plant cover (Calvo-Cases et al., 1991a,b; Calvo and Harvey, 1996; Solé-Benet et al., 1997).

As most of the sediments produced from the Tabernas badlands come from steep bare, S and W oriented slopes (Calvo and Harvey, 1996; Solé-Benet et al., 1997), with a very thin soil and/or regolith (Fig. 1), it is important to know the magnitude and the



Fig. 1. General view of a representative SW oriented slope in the badland area of Tabernas (shrub height about 40 cm). A real time image from a web cam can be accessed at <http://cautivo.eeza.csic.es>.

variability over time of the weathering processes, as well as their leading causes, in order to estimate weathering rates and sediment yield under present climatic conditions. Such knowledge is also important for the prediction of future erosion rates and for erosion control. An additional interest lies in understanding the processes, which produce the small scale landform characteristics of this mudstone area. This particular landscape is legally protected (as Paraje Natural) because of its remarkable scenic value.

Goudie (1989), in a comprehensive review of weathering processes in arid areas, indicates that arid zones are not zones of geomorphological inactivity. In the Tabernas Desert, two of the main factors reported by Goudie (1989) as contributing to rock weathering seem to happen simultaneously: moisture alternations and salt crystallisation and hydration. The origin of the salts in the study site is the in-situ parent material, a gypsiferous mudstone.

In order to verify the effectiveness of the two main weathering factors in this area and to describe the consequences of the weathering processes in detail, a double experimental approach using both laboratory and field-based techniques was undertaken on these materials.

(a) Fresh mudstone blocks were subjected to wetting–drying cycles in the laboratory with a view to obtaining qualitative and quantitative data about the number of cycles and the dissolved salts which might control weathering processes.

(b) Field weathering plots were established with a view to quantifying the weathering rate of a consolidated mudstone outcropping at the bottom and sides of gully channels.

## 2. Methods

### 2.1. *Characterisation of the mudstone and weathered regolith in a fresh terrain exposure*

A regolith profile was sampled from an exposure dug within El Cautivo instrumented catchment, 37°01'N–2°24' W, from the fresh mudstone to the surface. Samples were taken from three depths (0–1, 5–10, and 10–20 cm) and the following parameters for regolith and mudstone characterisation, as in Solé-Benet et al. (1992), were obtained: mineralogical composition (X-ray diffraction), Atterberg limits, particle-size distribution (pipette method), pH and electrical conductivity of the saturated paste, CaCO<sub>3</sub> equivalent (acidimetry), and total gypsum equivalent (Porta, 1998). The water coherence test was determined according to Emerson (1967). Total porosity and pore size distribution were also measured (Hg-intrusion porosimetry).

### 2.2. *Laboratory experiment*

For mudstone characterisation, a single large piece of fresh mudstone was also extracted near the exposure. From this piece, 10 blocks were dry-cut to fit into

aluminium boxes  $20 \times 10 \times 5$  cm (Fig. 2) without bottoms or lids. The blocks were cut without taking into account the natural orientation of the mudstone under field conditions. A piece of cloth (50% cotton–50% polyester) was fixed at the bottom of every box to allow water in and out of the blocks while retaining possible detached particles from the mudstone. The empty space between the block and the aluminium walls of the box was filled with an impervious polyurethane foam (Fig. 2), with two aims: to ensure that capillary water would flow only through the mudstone, and to provide sufficient resistance to every sample for easy handling. A similar sampling and handling technique had previously been used to study the experimental weathering of a Cretaceous mudrock in NE Spain (Regüés et al., 1993, 1995; Pardini et al., 1995).

The wetting–drying cycles consisted of the following procedures: first, the samples, numbered 1–10, were dried in an oven at  $40^\circ\text{C}$ , up to constant weight; thereafter, the samples were placed in sand baths saturated with distilled water until the whole surface of the blocks appeared wet; at that moment, the samples were weighed. Throughout the wetting phase, the laboratory temperature was kept at  $25^\circ\text{C}$ .

Three sets of two boxes, six boxes in total, underwent 5, 10 and 20 wetting–drying cycles (samples 1 and 2, 3 and 4, 5 and 7, respectively). Two boxes (6 and 9) remained as controls. Throughout the experiment, sample 8 remained dry at  $40^\circ\text{C}$  while sample 10 was placed in a permanently saturated sand bath. In this latter case, distilled water had to be added periodically to compensate for evaporation losses from both the sample itself and the sand. The  $40^\circ\text{C}$  temperature for the oven was chosen for three reasons: to accelerate drying, to simulate near maximum air temperatures in the Tabernas Desert, and to minimise the impact of induced mineralogical transformations of gypsum (i.e. gypsum to bassanite) and of other possible minerals.

After 5, 10 and 20 cycles, respectively, every block was carefully cut into two sub-samples, one for “undisturbed” analysis (morphology and micromorphology) and the other for “destructive” analysis (chemistry and mineralogy).

After oven drying at  $40^\circ\text{C}$ , undisturbed samples were impregnated with an unsaturated polyester resin under vacuum. Thin sections were then prepared from every sample

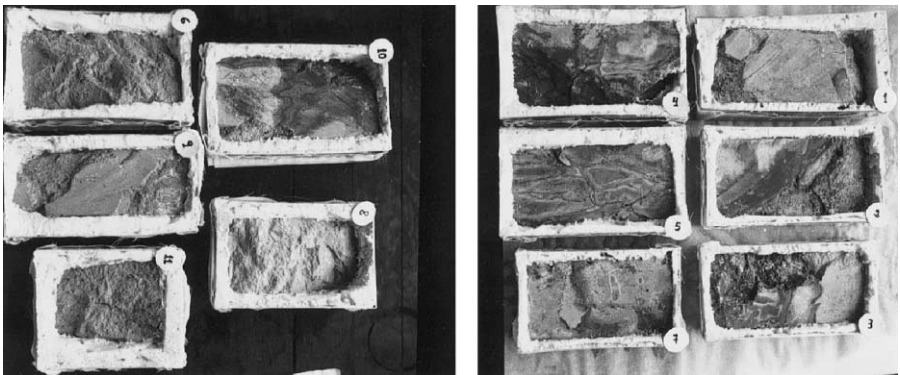


Fig. 2. Undisturbed mudstone blocks within aluminium boxes (boxes numbered 1, 2, 3, 4, 5, 6, 7, 9 and 10 measure about  $20 \times 10$  cm); the mudstone is isolated from the box walls by polyurethane foam.



Fig. 3. Weathering plots (50×50 cm) equipped with Gerlach troughs to collect water and sediments, which are conveyed to a PVC jug.

for further description under the polarising microscope, following procedures from Bullock et al. (1985).

Mineralogical and chemical analyses were performed on both the efflorescences which had emerged at the surface of some blocks, removed by scratching them with a sharp knife and further sweeping with a fine brush, and from different layers within the block: from 0 to 1, from 1 to 10, and from 20 to 40 mm depths.

Mineralogical analyses were carried out on powders by means of X-ray diffraction with a Cu target tube and a graphite monochromator, using the net intensities of the integrated area of the characteristic peak of each identified mineral for quantitative calculations (Chung, 1974).

The elemental chemistry of the samples was investigated by radioisotope induced X-ray fluorescence (RIXRF), with three different radioisotope sources ( $^{55}\text{Fe}$ ,  $^{109}\text{Cd}$  and  $^{241}\text{Am}$ ), and Si (Li) detector covering elemental detection in the range from Al to U. All the samples were analysed and spectral data recorded for further comparison.

Soluble salts were investigated on 1:5 crushed mudstone–water extracts by means of Atomic Absorption Spectrophotometry, for  $\text{Ca}^{2+}$ ,  $\text{Mg}^{2+}$ ,  $\text{Na}^+$  and  $\text{K}^+$ , and Ion Chromatography, for  $\text{Cl}^-$ ,  $\text{SO}_4^{2-}$ , and  $\text{HCO}_3^-$ .

### 2.3. Field (weathering plots)

Two bounded plots,  $50 \times 50$  cm, were set over a freshly dismantled mudstone (Fig. 3). The relatively smooth surface had a slope gradient of  $15^\circ$  and Gerlagh troughs were installed on the lower parts to collect runoff and sediments (weathered detached material), which were conveyed to a PVC jug. In one plot (P1), the surface was left untouched for 45 months and in the other plot (P2), approximately every 6 months, the surface was brushed and the sediments collected were dried, weighed and added to those from the jug.

Rainfall data over the 45-month period of field monitoring, were obtained in situ (meteorological station of El Cautivo Experimental Site). Only rainfall events larger than 3 mm have been considered, as other studies in the site have revealed that this is the threshold for detectable increases in soil or regolith water content (Cantón, 1999; Cantón et al., submitted).

## 3. Results

### 3.1. Characterisation of a natural weathering sequence

In the Tabernas landscape, fresh mudstone outcrops only at the bottom and sides of channels. However, the bare, thin regolith which covers most S- to W-facing slopes constitutes about 35% of the area. A representative fresh exposure provided the regolith profile for this characterisation.

Selected properties of the mudstone and the regolith are shown in Table 1. As was stated by Solé-Benet et al. (1997), the mudrock is formed mainly of silt grains (80%)

Table 1

Characterisation of a natural weathering profile. Depth of samples: TA0101 = 0–1 cm; TA0102 = 5–10 cm; TA0103 = 10–20 cm. EC = electrical conductivity; LL = liquid limit, PL = plastic limit; IP = plasticity index

	CaCO <sub>3</sub> (%)	Gypsum (%)	pH	E.C. (dS m <sup>-1</sup> )	Atterberg limits			Particle size, with CO <sub>3</sub> <sup>2-</sup> (%)					Particle size, without CO <sub>3</sub> <sup>2-</sup> (%)					
					LL	PL	IP	Coarse sand	Fine sand	Coarse silt	Fine silt	Clay	Coarse sand	Fine sand	Coarse silt	Fine silt	Clay	
TA0101	26.86	14.3	7.68	2.09	32	22.7	9.3	n.a.	n.a.	n.a.	n.a.	n.a.	n.a.	n.a.	n.a.	n.a.	n.a.	n.a.
TA0102	24.22	15.03	7.71	3.56	33.4	22	11.4	0.06	13.2	33.59	48.56	4.65	0.05	10.22	27.07	54.51	8.14	
TA0103	28.22	9.38	7.79	5.79	31.4	22	9.4	0.05	13.5	32.75	49.53	4.19	0.07	13.14	29.18	50.51	7.1	

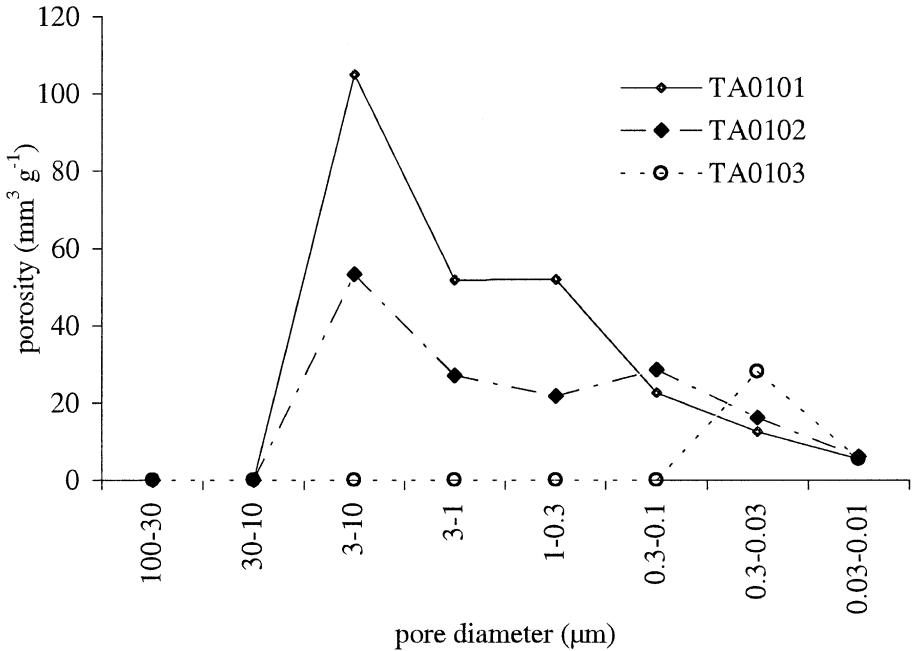


Fig. 4. Hg-intrusion porosimetry of samples from a weathering profile. Identification and total porosity ( $\text{mm}^3 \text{g}^{-1}$ ): TA0103 = third, deepest layer, fresh mudstone (33.72); TA0102 = second layer (131.15), TA0101 = upmost, surface layer (250.25).

with the following mineralogical composition: muscovite 35%, paragonite 10%, minerals with a main peak at 1.4 nm (mainly chlorite and a small proportion of smectite) 3%, quartz 9%, calcite 20–35%, dolomite 2–5% and gypsum 5–20%. In the weathering profile, an upwards decreasing trend in soluble salts (expressed as electrical conductivity) is observed, while the pH remains constant. The index of plasticity of the material, around 10, combined by a relatively low liquid limit (31%) indicates its high potential to produce mass movements, provided enough water is available, conditions which do not occur very often, given the climatic conditions of the area.

Also, the Emerson (1967) test for aggregate stability indicates that the material belongs to class 2, very unstable: it rapidly disintegrates into primary particles when submerged in distilled water.

Hg-intrusion porosimetry shows how upon weathering, total porosity progressively increases, from  $33.72 \text{ mm}^3 \text{g}^{-1}$  (9% of rock volume) in the fresh mudstone to  $250.25 \text{ mm}^3 \text{g}^{-1}$  (66% of rock volume) in the surface regolith, as well as the dominant size of pores becoming progressively larger (Fig. 4).

### 3.2. Experimental weathering

#### 3.2.1. Morphological–micromorphological analysis

After cutting, the blocks at the end of the experiment, two features were noted: the upper exposed-surface and the cross-section of the blocks.



*3.2.1.1. Upper surface.* After five wetting–drying cycles, a very thin layer (of the order of 0.1 mm) of efflorescences was observed at the surface of all replicated blocks. After 20 wetting–drying cycles, the efflorescence layer had increased up to 1 mm. The permanently saturated sample presented the largest efflorescence concentration, with a thickness of more than 1 mm (see below for chemical and mineralogical composition). Control samples and the one permanently at 40°C produced no efflorescence.

*3.2.1.2. Cross-section.* The analysis of the cross-sections from control samples shows a quite homogeneous groundmass but a heterogeneity in the amount and size of cracks and fissures. This last feature must certainly influence the ease with which water can penetrate and circulate through the material, influencing salt dissolution rates. Under the microscope, cracks are either completely or partially filled with densely packed, pure (clean) gypsum crystals perpendicularly oriented to pore walls (Fig. 5). This gypsum, while secondary in origin because of natural diagenetic processes (both sedimentary burial and deep weathering) will be considered as primary in this study as opposed to secondary gypsum, which is formed as a consequence of surface weathering, specifically during the present experiment.

Cross-sections from wetted-dried samples also show homogeneous ground-masses but a progressive (along with the number of wetting–drying cycles) and considerable

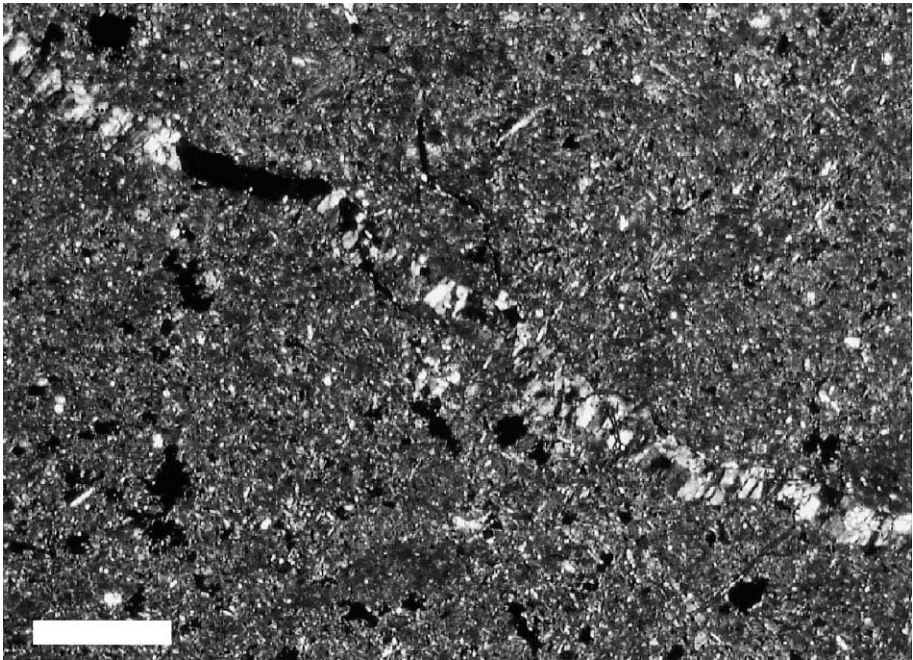


Fig. 5. Micrograph of thin section (under cross-polarised light) of an undisturbed fresh mudstone. Observe the crack (going from upper left to bottom right) filled with gypsum. Scale bar = 1 mm.

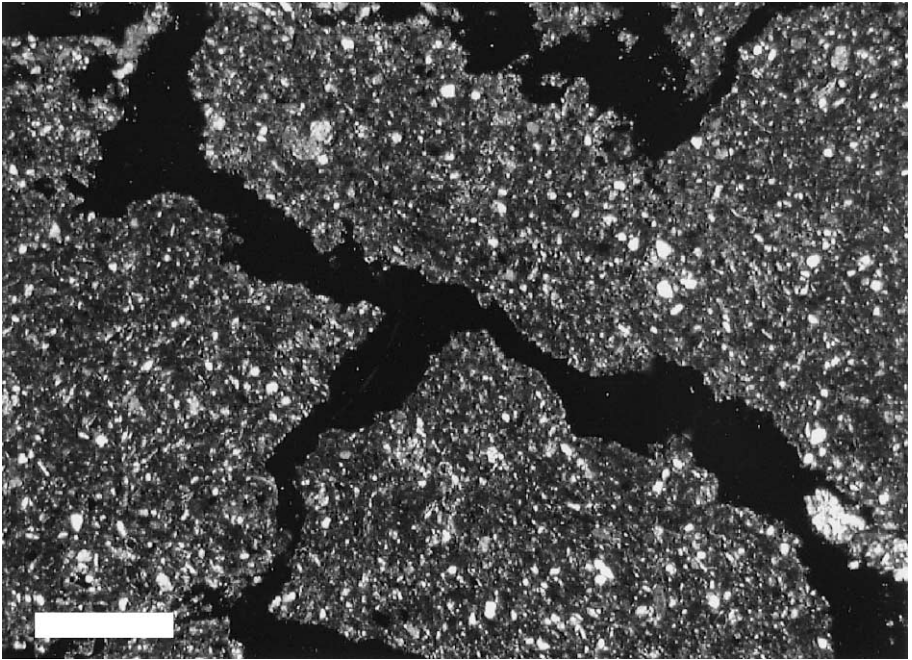


Fig. 6. Micrograph of thin section (under cross-polarised light) of a weathered mudstone after 20 wetting–drying cycles. Almost no gypsum remains within the cracks (only some is visible at the bottom right-hand corner). Scale bar = 1 mm.

increase in the amount and size of cracks in relation to the control samples. Most of the gypsum filling diagenetic or postdiagenetic cracks, have mostly disappeared (Fig. 6). The higher the number of wetting–drying cycles, the higher the degree of shattering.

Differences in the main direction of cracks within block 5 and block 7 (Fig. 7), both subjected to 20 wetting–drying cycles, might be due to differences in orientation with regard to initial sedimentary layering, as the mudstone blocks were cut at random. The fact that different moistening directions within the mudstone leads to similar cracking patterns may also indicate that regardless of the moistening direction, either vertical or horizontal, the resulting weathering is quite similar.

### 3.2.2. Weight analysis

The succession of dry and wet weights for all the samples (5, 10 and 20 wetting–drying cycles) produces three clear results as the number of wetting–drying cycles increases: (a) the dry weights progressively decrease; (b) the wet weights progressively increase; and (c) the amplitudes between the dry and the wet weights progressively increase (Fig. 8).

The first result indicates a progressive loss of weight, which must be due either to the loss by dissolution of some soluble mineral (salts) within the sample in the wetting

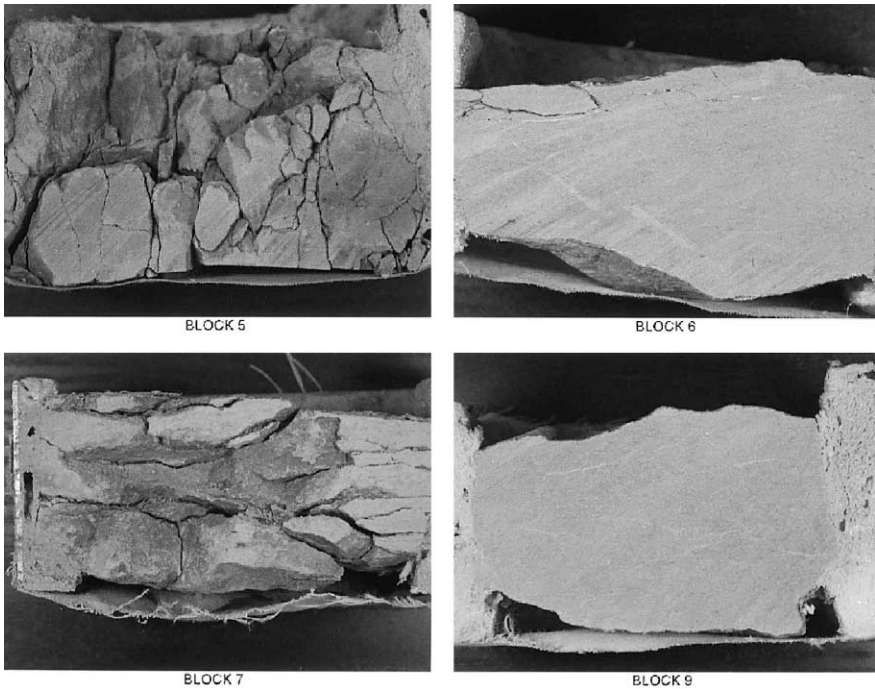


Fig. 7. Sections of weathered and fresh mudstone blocks (approximately  $10 \times 5$  cm). At right, control samples No. 6 and No. 9 (fresh mudstone); at left, after 20 wetting–drying cycles, samples No. 5 and No. 7.

phase or by the enhanced dehydration of some mineral (salts, mainly gypsum) as a consequence of oven heating. The second result is a consequence of the first: when water dissolves salts, some new pore space increases the water intake in the following saturation phase. The third result is a logical consequence of two previous results: this progressive enlargement of pre-existing pore volume may enhance further weathering through solution.

The differences between wet and dry weights in each cycle may be considered as most of the pore volume available for water absorption (probably not far from the water absorption capacity, calculated as the difference between the weights at full saturation and at  $105^\circ\text{C}$ ). The former value will be called “ $\beta$ -water absorption”. The pore volume considered is attributed to micro-porosity because it is exclusively related to capillary water. Plotting the  $\beta$ -water absorption values from all samples and cycles, we observe that all the samples follow a similar evolution, the data for which may be adjusted to a potential best fit curve (Fig. 9):

$$y = 9.9622 x^{0.2712}, \quad r^2 = 0.9025,$$

indicating that the most important micro-pore enlargement occurs in the first few cycles of the wetting–drying process.

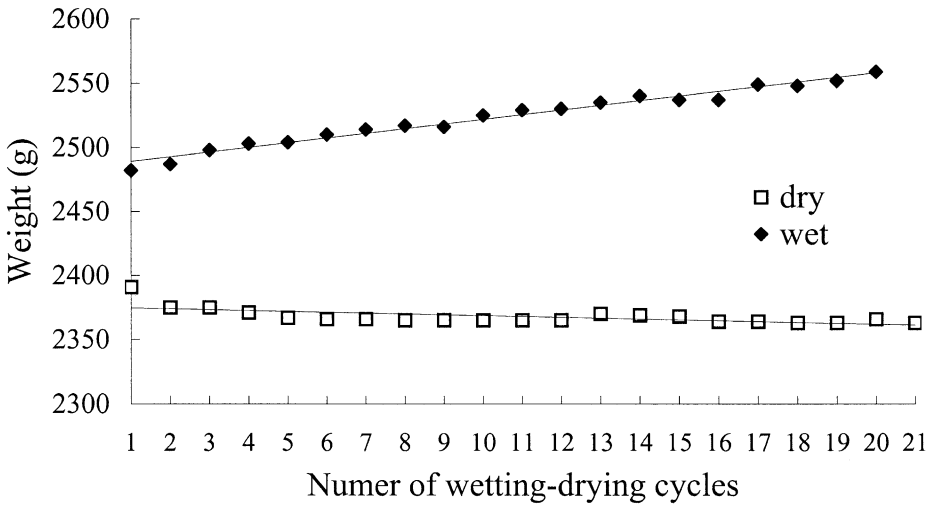


Fig. 8. Successive weights of sample No. 5 after every drying and wetting treatment until 20 cycles were completed. Observe the increasing trend of the wet weights and the decreasing trend of dry weights.

3.2.3. Chemistry

3.2.3.1. Total elements. The samples from the 20–40 mm layer, from all treatments, show the presence of Si, K, Ca, Ti, Mn, Fe and S as main elements, and the presence of Zn, Rb, Sr, Zr, Ba, La, Ce, and Nd, as trace elements.

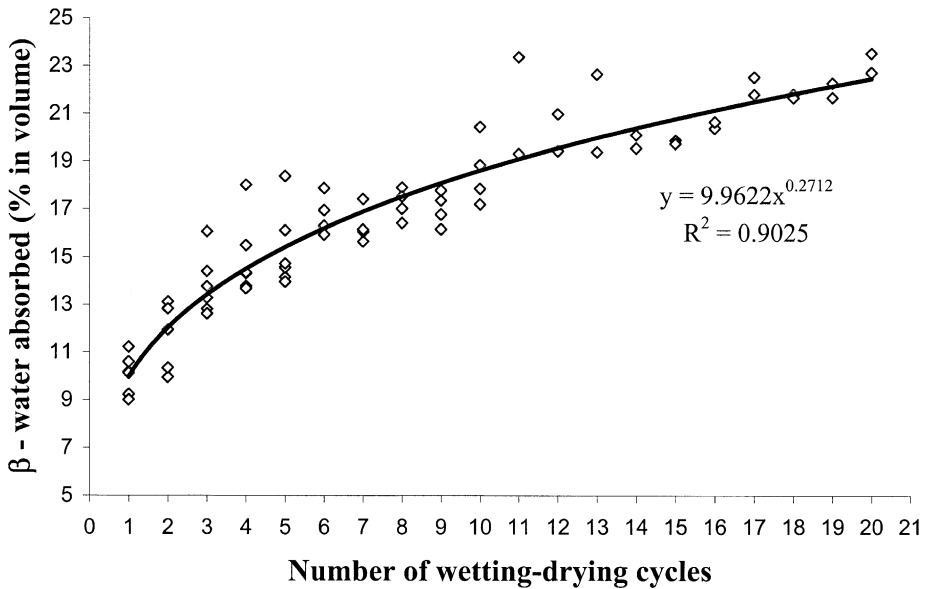


Fig. 9. β-water absorbed of all experimental blocks in every wetting–drying cycle and best-fitting model.

From the spectra obtained by means of irradiation using the  $^{55}\text{Fe}$  source (light elements), an increase of S content from the inner layers (20–40 mm) to the surface (efflorescences) can be observed, interpreted as a typical S migration towards the surface. This behaviour is observed in all wetted–dried samples.

Elements heavier than Ca do not reveal a single and common behaviour in all the samples studied. As an example, a comparison between sample 2 (five cycles) and sample 10 (permanently saturated) is given: a clear decrease in Sr, Rb, Zr, Fe, Ba and rare earth elements from the inner layer (20–40 mm) to the efflorescences was observed in both sample 2 and sample 10, except for Sr, which exhibits an inverse trend (increasing towards the efflorescence).

Table 2

Soluble ions (in  $\text{cmol l}^{-1}$ ) extracted from 1:5 solid–water from the crushed sub-samples from the blocks at the end of the experiment. Sub-samples within every block: a = 0–1 mm depth from the surface; b = 1–10 mm; c = 20–40 mm

Treatment	Sample	Sub-sample	Ca <sup>2+</sup>	Mg <sup>2+</sup>	Na <sup>+</sup>	K <sup>+</sup>	Cl <sup>-</sup>	SO <sub>4</sub> <sup>2-</sup>	HCO <sub>3</sub> <sup>-</sup>	Σ cations	Σ anions	
5 Cycles	1	a	4.00	4.33	8.78	0.51	0.91	9.92	2.75	17.63	13.58	
		b	7.20	2.50	3.57	0.41	4.89	6.50	1.40	13.68	12.79	
		c	2.80	2.17	1.48	0.41	0.00	6.83	0.25	6.86	7.07	
	2	a	10.10	9.67	7.39	0.51	6.96	17.68	1.60	27.67	26.23	
		b	8.70	3.00	4.17	0.41	5.75	9.49	0.25	16.28	15.49	
		c	5.10	4.17	2.52	0.36	4.43	6.04	2.00	12.15	12.47	
	10 Cycles	3	a	6.20	8.17	13.91	1.03	8.31	20.81	2.69	29.31	31.81
			b	9.10	4.00	3.04	0.51	7.93	7.61	1.15	16.66	16.69
			c	8.40	3.33	2.17	0.41	7.69	5.67	1.52	14.32	14.88
4		a	7.60	4.50	7.48	0.67	6.00	12.32	2.49	20.24	20.81	
		b	14.50	4.00	3.57	0.46	14.71	7.29	1.25	22.53	23.24	
		c	10.50	5.67	1.83	0.41	5.87	12.00	1.30	18.40	19.17	
20 Cycles	5	a	4.00	6.33	13.91	0.51	7.29	16.60	0.87	24.76	24.77	
		b	5.30	3.00	3.13	0.46	0.00	10.56	1.37	11.89	11.94	
		c	1.20	1.50	1.39	0.31	0.00	3.17	1.37	4.40	4.54	
	7	a	12.50	9.50	11.91	0.97	10.15	24.06	0.75	34.89	34.95	
		b	5.50	6.17	2.26	0.87	0.02	13.97	1.02	14.80	15.02	
		c	1.10	1.67	1.13	0.36	0.00	3.08	1.30	4.26	4.38	
Control	6	a	8.80	2.83	4.96	0.36	2.94	10.53	1.90	16.95	15.37	
		b	6.70	3.17	6.17	0.41	1.67	10.33	1.10	16.45	13.09	
		c	6.90	3.67	7.48	0.62	1.90	13.82	1.07	18.66	16.79	
	9	a	3.40	3.67	4.26	0.36	1.49	8.68	1.65	11.69	11.82	
		b	5.40	3.83	4.96	0.36	0.00	11.76	1.20	14.55	12.96	
		c	3.90	3.50	4.78	0.41	0.00	10.69	1.60	12.59	12.29	
40°C	8	a	8.50	2.83	6.09	0.51	2.17	11.92	0.12	17.93	14.22	
		b	4.70	3.00	6.17	0.46	1.22	10.22	1.10	14.34	12.54	
		c	6.30	3.17	5.48	0.46	1.35	12.82	1.40	15.41	15.57	
Saturated	10	a	0.20	1.00	1.39	0.21	0.00	0.00	2.90	2.80	2.90	
		b	4.00	1.67	1.04	0.36	0.00	4.79	1.32	7.07	6.12	
		c	4.00	4.17	2.70	0.51	0.00	11.46	1.27	11.38	12.73	

**3.2.3.2. Soluble salts.** Total efflorescences were removed and weighed at the end of three sets of wetting–drying cycles. The rates between the weights of the efflorescences and the weights of their corresponding blocks increase with the number of cycles: 0.02% (blocks 1 and 2, 5 cycles), 0.10% and 0.17% (blocks 3 and 4, respectively, 10 cycles), and 0.44% (blocks 5 and 7, 20 cycles) and reaches 0.75% on the permanently saturated sample, indicating in all cases an important migration of soluble salts, and also a proportional migration to the number of wetting–drying cycles.

Once the efflorescences were removed, the solid blocks were also analysed for their remaining content of soluble salts. The salts extracted from three layers from the samples subjected to either wetting–drying cycles or permanent water-saturation indicate significant ion mobility. In the control samples, some heterogeneity is observed, as in the morphological description (Section 3.2.1.2). In Table 2, significant differences can be appreciated from depths *a–c* in wetted–dried samples and an upwards or bottom-up migration is proportional to the number of wetting–drying cycles. In permanently wet samples, a reverse trend, or downwards migration is observed.

Whatever the direction of salt concentration, either upwards (migration is mainly driven by evaporation from the top while wetting with distilled water comes from the bottom) or downwards (once the sample is wet, the ionic equilibrium with the wetted sand bath occurs through an ionic migration towards the less concentrated solution), the important fact is the magnitude of ionic migration which is indicative of a considerable dissolution of some mineral components of the mudstone.

#### 3.2.4. Mineralogy

Main results of the mineralogical analyses are detailed in Tables 3 and 4.

Much caution should be used in the interpretation of the results on efflorescences due to the changing nature of sulphates in variable environmental conditions; it is not possible to detail in situ transformations during and after the experiment. X-ray diffraction can be used to identify gypsum; however, its use for the quantitative determination of gypsum is usually inaccurate unless a complex and tedious procedure is used (Skarie et al., 1987 cited by Porta, 1998).

The efflorescences at the surface of the samples are composed mainly of sulphates. We can distinguish four different mineralogical types: gypsum,  $\text{CaSO}_4 \cdot 2\text{H}_2\text{O}$ , bassan-

Table 3

Mineralogical composition of efflorescences in all samples subjected to wetting–drying cycles and to permanent saturation. Data represent intensities of the main peak of every mineral. w–d = wetting–drying

Sample	w–d cycles	Bassanite	Hexahydrate	Loeweite	Gypsum
1	5	412	–	103	–
2	5	898	–	105	–
3	10	309	184	282	–
4	10	272	151	271	–
5	20	208	–	92	1168
7	20	143	–	75	504
10	saturation	1030	271	321	208

Table 4

Bulk sample mineralogy from the most representative samples of the experiment. Data represent intensities of the main peak of every mineral. w–d = wetting–drying

Sample	w–d cycles	Chlorite	Muscovite	Paragonite	Quartz	Gypsum	Calcite	Dolomite
<i>Layer 0–1 mm</i>								
1	5	225	1404	370	506	566	1830	334
2	5	218	1510	359	500	2801	1590	325
5	20	367	2790	574	587	874	1890	322
7	20	353	3381	691	605	931	1834	401
9	Control	275	2056	464	500	235	1967	332
10	Saturation	281	1780	440	530	1157	2030	286
<i>Layer 20–40 mm</i>								
1	5	316	1999	516	501	297	2220	463
2	5	279	1989	423	550	437	2079	340
5	20	309	2060	503	526	479	2030	295
7	20	336	2166	586	576	–	1878	238
9	Control	221	1216	337	539	317	2290	318
10	Saturation	350	2946	623	542	–	2174	339

ite,  $\text{CaSO}_4 \cdot 0.5\text{H}_2\text{O}$ , hexahydrate,  $\text{MgSO}_4 \cdot 6\text{H}_2\text{O}$ , and loeweite,  $\text{Na}_{12}\text{Mg}_7(\text{SO}_4)_{13} \cdot 15\text{H}_2\text{O}$ .

Some differences among the samples related to the number of wetting–drying cycles can be recognised. Bassanite and loeweite are common structural types in all the efflorescences. Those subjected to 10 cycles exhibit the presence of hexahydrate while a more extended cycling leads to the formation of gypsum without hexahydrate. The efflorescences of the permanently saturated sample (10) reveal the presence of all four minerals.

The bulk samples have a relative simple composition: muscovite, paragonite (the Na-rich equivalent of muscovite), and chlorite, as phyllosilicates, calcite and dolomite as carbonates, and gypsum as the only sulphate. Using the Chung (1974) method for mineralogical quantification, an overestimation of calcite and dolomite as well as a clear underestimation of gypsum is observable when comparing with chemical analysis, due to the inaccuracy of the X-ray diffraction technique used for gypsum quantification (Skarie et al., 1987).

Comparison between samples of the 20–40 mm depth layer and those from the surface layer reveal heterogeneity in the mineralogical composition of control samples, as well as a noticeable increase in gypsum content towards the surface in treated samples.

Because of the existence of minerals composed of sodium and magnesium sulphates in the efflorescence layer, minor amounts of these minerals, although undetected by XRD, might also be assumed to be present in the internal layers of the samples. The crystallisation of small amounts of such minerals is known to play an essential role in the mechanical weathering of rocks (Goudie, 1989). A similar consideration might be applied to bassanite, detected only in the efflorescence layer: if present in inner layers, its hydration to gypsum would represent another existing salt weathering process.

No chlorides were detected with XRD, although the chemical analysis of soluble anions has revealed the presence of chlorides, which might have originated from halite (NaCl).

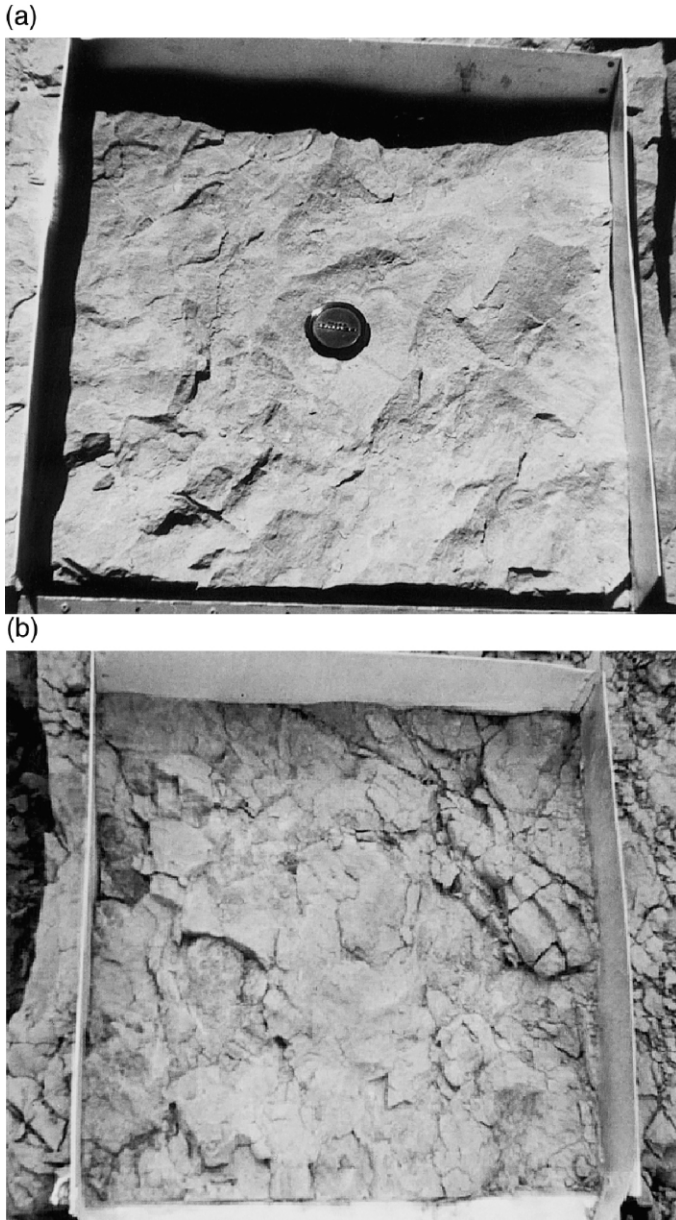
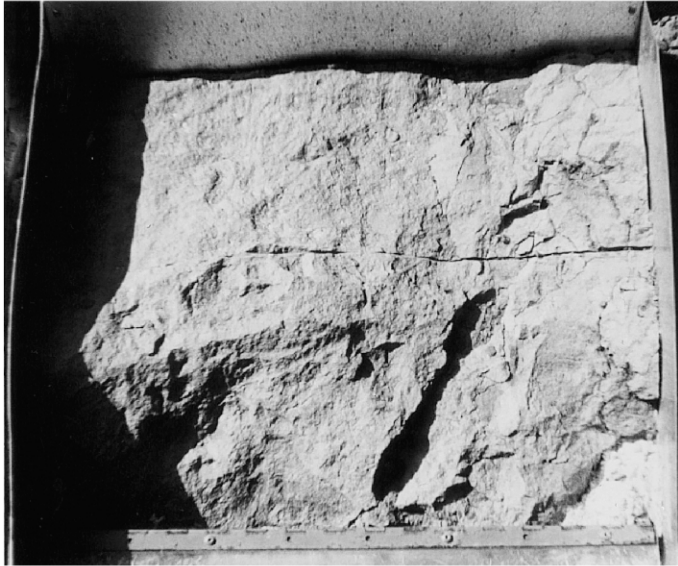


Fig. 10. Plot 1 (control) (a, b) and plot 2 (c, d) at the beginning (a, c) and at the end (b, d) of the 3-year experiment. Bounded plots are 50×50 cm.



(c)



(d)



Fig. 10 (continued).

### 3.3. Field plots

After 3 years of exposure to surface weathering agents, the surface pattern of the experimental plots had significantly changed (Fig. 10b and d) with regard to the original

Table 5

Weathering production at intervals of about six months, total rainfall and number of rainfall events higher than 3 mm, during these periods

Sampling dates	Exported sediments (g)	Rainfall (mm)	Rainfall events > 3 mm
6/7/95	beginning of the experiment		
17/1/95	716	80	5
23/6/95	1144	69	5
19/1/96	3194	202	10
9/7/96	3187	112	11
15/1/97	1833	178	13
2/6/97	641	87	6
1/3/98	632	188	4
Total	11,346	916	54

surface (Fig. 10a and c). After 3 years, a high degree of shattering can be observed on both plots. The evolution of sediment yields through time, as well as the total output at the end of the 3-year period are presented in Tables 5 and 6. In plot 1, where the weathered, detached particles were not removed from the mudstone surface during the 3-year period, the final sediment yield reaches  $1.79 \text{ kg m}^{-2} \text{ year}^{-1}$ , or  $0.68 \text{ mm year}^{-1}$ , while in plot 2, with repeated removal of the detached weathered material after main rainfall events (natural runoff plus sweeping the plot surface with a soft brush), sediment yield is  $12.45 \text{ kg m}^{-2} \text{ year}^{-1}$ , corresponding to a breakdown rate of  $4.71 \text{ mm year}^{-1}$  (Table 6).

The average sediment yield per approximately 6-month sampling interval, is  $1621 \pm 470 \text{ g}$ . However, we observe (Table 5) two groups of sampling intervals in which sediment yields are either considerably below the average (783 g) or considerably above (2738 g), and these groups are related to the number of rainfall events larger than 3 mm which occurred during those periods. An ANOVA indicates a significant ( $p < 0.05$ ) relationship between sediment yield and the number of rainfall events, suggesting the importance of the number of wetting–drying cycles in the production of detachable material.

When the removal of detached particles is more aggressive (removing all detached shards), sediment yield for plot 2 reaches  $20.74 \text{ kg m}^{-2} \text{ year}^{-1}$ , or  $7.89 \text{ mm year}^{-1}$  (Table 6). The two methods of sediment removal can be considered as minimum and maximum figures for sediment yields from the natural weathering of the mudstone.

Table 6

Sediment yield and erosion rates at both plots (P1 and P2)

	Sampling method	Sediment yield ( $\text{kg m}^{-2} \text{ year}^{-1}$ )	Erosion rate ( $\text{mm year}^{-1}$ )
P1	mild	1.79	0.68
	aggressive	9.06	3.44
P2	mild	12.45	4.7
	aggressive	20.74	7.89

All this indicates that the removal of weathered material favours further weathering or, stated otherwise, that a mantle of weathered debris protects the fresh mudstone from both weathering and erosion. Given the low infiltration in this environment (Alexander et al., 1994; Calvo and Harvey, 1996; Solé-Benet et al., 1997), deep weathering should not be very important, as shown by Cantón (1999). However, the bottom and sides of channels where runoff periodically scours the layer of weathered mudstone, might have incision rates similar to the weathering rates presented above.

#### 4. Discussion and conclusions

Despite the heterogeneity assessed from different analytical techniques on the control samples, significant trends in pore enlargement and anion migration have become apparent as the result of a few wetting–drying cycles. Neither the possible consequences of associated temperature cycling, from 25°C to 40°C, nor the process of swelling–shrinking because of the relatively low clay content, has been considered in this experiment. Their effect might contribute to pore enhancement and thus remains to be studied.

From the results obtained, it must be emphasised that micro-porosity significantly increases in the first five wetting–drying cycles. However, the number and size of cracks (attributed to macro-porosity because they are mainly wider than 100  $\mu\text{m}$ ) are better developed after the 20 wetting–drying cycles. This is probably associated with the observation that a new generation of cracks and fissures develops after each wetting–drying cycle and widens the previous generation of cracks and fissures. This results in a progressive widening of cracks and fissures as the number of wetting–drying cycles progresses, creating a weathered mass of surface regolith composed entirely of mudstone shards, as is observed in a natural regolith profile.

In the first wetting cycle the fresh mudstone, with a total porosity of around 9%, absorbs about 9% of water, indicating quite a compacted and impervious material. After 20 wetting–drying cycles, the amount of absorbed water reaches up to 23% (Fig. 9).

Crystallisation pressures from previously dissolved salts or from other weathered minerals within mudstone pores are of paramount importance in the disaggregation of rocks. Winkler and Singer (1972) report for gypsum and anhydrite crystallisation pressures from 282 to 1900  $\text{kg cm}^{-1}$  (from 0°C and a degree of super saturation of 2, to 50°C and a degree of super saturation of 50) and from 118 to 300  $\text{kg cm}^{-1}$ , respectively. Halite has even higher crystallisation pressures, ranging from 554 to 3737  $\text{kg cm}^{-1}$  (under the same conditions as above).

Salt migration is an important weathering process related to the formation and/or widening of cracks and fissures, which can transmit additional water for further salt solution and/or crystallisation. Upon drying, salts migrate towards the surface and crystallise either as efflorescences or inside the mudstone, contributing to pore enhancement and subsequent mudstone fragmentation. A particular feature, in the permanently saturated sample, has been the migration of salts towards the lower salt concentration of the sand bath, in the opposite direction to all other wet-dried samples.

The presence of bassanite suggests that at least part of the calcium sulphate is not completely hydrated, and consequently is a potential agent for further weathering upon hydration.

This study shows the significant relationship found under field conditions between the number of rainfall events higher than 3 mm and the amount of detached, weathered material. This weathered material results from the progressive increase in pore volume assessed under laboratory conditions, due both to the dissolution of salts and to further crystallisation within cracks and fissures.

There are geomorphological implications for the Tabernas Desert at several scales, allowing us to understand the erosion mechanisms for these badlands.

At the small plot scale, because of the low annual precipitation of the area and the small number of rainfall events larger than 3 mm (about  $8 \text{ year}^{-1}$ ), wetting–drying cycles in the upper few millimetres of marls can occur easily but are limited in depth by the lack of infiltration (Calvo-Cases et al., 1991a,b; Alexander et al., 1994; Solé-Benet et al., 1997). In wet years, however, with rainfall events higher than 20 mm, infiltration fronts can go somewhat deeper and consequently have higher weathering impact.

Following Carson and Kirkby (1972), in the Tabernas Desert, a general transport-limited condition exists. On SW oriented slopes, where erosion is visible and apparently rapid, in wet years (Calvo-Cases et al., 1991a,b; Alexander et al., 1994), with a relative high number of wetting–drying cycles, a regolith a few decimetres thick is formed and when occasional high intensity rainstorms occur, only part of the unconsolidated material is eroded from hillslopes. On NE oriented slopes, where erosion is apparently slower and less visible because of a generalised plant cover (lichens and disperse annual and perennial plants), infiltration has formed a considerable weathered mantle, which only on rare occasions is partially subjected to mass movements, rilling or gullying (Calvo-Cases et al., 1991a,b; Alexander et al., 1994).

In a context of climatic change, if there were to be a decrease in the number of rainfall events, and consequently in the number of wetting–drying cycles, but an increase of rainfall intensity, a possible weathering-limited condition might develop.

This study has established on the basis of sequential field observations that the amount of sediment depends on the antecedent weathering, the number of wetting–drying cycles and the rainfall magnitude which controls infiltration depth.

In the Tabernas desert, the combined effect of moisture cycling and salt dissolution–precipitation constitutes an important weathering process which should be considered as a major environmental condition. Mudstone weathering must be taken into account not only in hydrological and geomorphological sediment yield studies, but also as a potential hazard in any civil engineering projects in the area.

## Acknowledgements

The research for this paper was carried out as part of collaborative research projects funded by both the European Commission and the Spanish CICYT, through their “Environmental Plan” and “Plan Nacional de I + D”, respectively (MEDALUS III — ENV4-CT95-0118, PROHIDRADE — AMB95-0986-C02-01, and Influencia del trans-

porte sólido en la calidad de los recursos hídricos — HID97-0581). The first author acknowledges a fellowship from the Dirección General de Investigación. The scientific agreement between CSIC and CNR financially supported exchange visits among Spanish and Italian researchers. Alfredo Durán is thanked for his help in setting the field plots. F. Domingo, M.A.Domene and M.J. Jorquera are thanked for assistance with chemical analysis. The property owner, the Viciano family, is specially thanked for granting permission to use their land as a “scientific experimental site”. Professors M. Thomas, A. Harvey and G. Stoops are kindly thanked for their constructive review of the manuscript.

## References

- Alexander, R.W., Harvey, A.M., Calvo, A., James, P.A., Cerda, A., 1994. Natural stabilization mechanisms on badland slopes: Tabernas, Almería, Spain. In: Millington, Pye (Eds.), *Environmental Change in Drylands: Biogeographical and Geomorphological Perspectives*. Wiley, pp. 85–111.
- Bullock, P., Fédoroff, N., Jongerius, A., Stoops, G., Tursina, T., Babel, U., 1985. *Handbook for Soil Thin Section Description*. Waine Research Publications, Wolverhampton, England.
- Calvo, A., Harvey, A.M., 1996. Morphology and development of selected badlands in SE Spain: implications of climatic change. *Earth Surf. Processes Landforms* 21, 725–735.
- Calvo-Cases, A., Harvey, A.M., Paya-Serrano, J., 1991a. Processes interactions and badland development in SE Spain. In: Sala, Rubio, García-Ruiz (Eds.), *Soil Erosion Studies in Spain*. Geofoma Ed., Logroño, Spain, pp. 75–90.
- Calvo-Cases, A., Harvey, A.M., Paya-Serrano, J., Alexander, R.W., 1991b. Response of badland surfaces in SE Spain to simulated rainfall. *Cuaternario y Geomorfología* 5, 3–14.
- Campbell, I.A., 1989. Badlands and badland gullies. In: Thomas, D.S.G. (Ed.), *Arid Zone Geomorphology*. Belhaven/Halsted Press, London, pp. 159–183.
- Cantón, Y., 1999. Efectos hidrológicos y geomorfológicos de la cubierta y propiedades del suelo en paisaje de cárcavas. PhD Thesis, Universidad de Almería, Spain.
- Cantón, Y., Domingo, F., Solé-Benet, A., Puigdefábregas, J. Hydrological and erosion response of a badlands system in semiarid SE Spain. *J. Hydrol.* (submitted).
- Carson, M.A., Kirkby, M.J., 1972. *Hillslope Form and Process*. Cambridge University Press, Cambridge.
- Chung, F.H., 1974. Quantitative interpretation of X-ray diffraction patterns of mixtures. I. Matrix-flushing method for quantitative multicomponent analysis. *J. Appl. Crystallogr.* 7, 519–525.
- Emerson, V.V., 1967. A classification of soil aggregates based on their consistence in water. *Aust. J. Soil Res.* 5, 47–57.
- Goudie, A.S., 1989. Weathering processes. In: Thomas, D.S.G. (Ed.), *Arid Zone Geomorphology*. Belhaven-Halsted, London, Chap. 2.
- Kleverlaan, K., 1989. Neogene history of the Tabernas basin (SE Spain) and its Tortonian submarine fan development. *Geol. Mijnbouw* 68, 421–432.
- Pardini, G., Pini, R., Barbini, R., Regüés, D., Plana, F., Gallart, F., 1995. Laser elevation measurements of a smectite-rich mudrock following freeze-tawing and wet-drying cycles. *Soil Technol.* 8, 161–175.
- Porta, J., 1998. Methodologies for the analysis and characterization of gypsum in soils: a review. *Geoderma* 87, 31–46.
- Regüés, D., Llorens, P., Pardini, G., Pini, R., Gallart, F., 1993. Physical weathering and regolith behaviour in a high erosion rate badland area at the Pyrenees: research design and first results. *Pirineos* 141/142, 63–84.
- Regüés, D., Pardini, G., Gallart, F., 1995. Regolith behaviour and physical weathering of clayey mudrock as dependent on seasonal weather conditions in a badland area at Vallcebre, Eastern Pyrenees. *Catena* 25, 199–212.

- Skarie, R.L., Arndt, J.L., Richardson, J.L., 1987. Sulfate and gypsum determinations in saline soils. *S.S.S.A.J.* 51, 901–903.
- Solé-Benet, A., Josa, R., Pardini, G., Aringhieri, R., Plana, F., Gallart, F., 1992. How mudrock and soil physical properties influence badland formation at Vallcebre (Pre-Pyrenees, NE Spain). *Catena* 19, 287–300.
- Solé-Benet, A., Calvo, A., Cerdà, A., Lázaro, R., Pini, R., Barbero, J., 1997. Influence of micro-relief patterns and plant cover on runoff related processes in badlands from Tabernas (SE Spain). *Catena* 31, 23–38.
- Winkler, E.M., Singer, P.C., 1972. Crystallization pressure of salts in stone and concrete. *Geol. Soc. Am. Bull.* 83, 3509–3514.